Vietnam Journal of Science and Technology ***56*** *(6) (2018) 698-705*

DOI: 10.15625/2525-2518/56/6/12722

MICROWAVE METAMATERIAL-BASED SUPERLENS FOR ENERGY FOCUSING APPLICATIONS

Kieu Vu Thang[1], Nguyen Thanh Tung[2, *], Ewald Janssens[3, **]

[1]*School of Physics, Hanoi University of Science and Technology, No 1 Dai Co Viet, Hai Ba Trung, Ha Noi, Viet Nam*

[2]*Institute of Materials Science, VAST, No 18 Hoang Quoc Viet, Cau Giay, Ha Noi, Viet Nam*

[3]*Laboratory of Solid State Physics and Magnetism, Department of Physics and Astronomy, KU Leuven, B-3001 Leuven, Belgium*

[*]Email: *tungnt@ims.vast.ac.vn,* [**]Email: *ewald.janssens@kuleuven.be*

Received: 5 July 2018; Accepted for publication: 4 September 2018

ABSTRACT

Superlens imaging has been known as one of the most intriguing applications of metamaterials due to its capability of sub-wavelength imaging. In this report, we numerically demonstrate the possibility to make an amplifying superlens, which can focus and consequently enhance electromagnetic signals emitted at GHz frequencies. Simulations using the finite integration technique are performed to explore the amplifying mechanism of the proposed superlens. It is found that the focused signals can be considerably intensified at a selected position. The results show potential uses of metamaterial superlenses for future wireless energy transfer devices and novel energy harvesting applications.

*Keyword***:** metamaterial, energy harvesting, superlens.

Classification numbers: 2.1.2, 3.4.1

1. INTRODUCTION

In recent years, increasing attention has been paid to metamaterials. This novel class of materials has fantastic electromagnetic features that do not exist in natural materials, including the negative refractive index, perfect absorption, and electromagnetically-induced transparency [1, 2]. The charming ability of metamaterials generally originates from their structure rather than from their composition. Metamaterials often are composed of periodically-arranged subwavelength electromagnetic resonators and each resonator can be considered as a “meta-atom”. By changing the sorting rules of these "meta-atoms", one can independently tailor the electric and magnetic responses of metamaterial media and this nearly at will. The most intriguing property of metamaterials, the negative refractive index, could be obtained for the first time in 1968 by simultaneously combining negative permeability $\mu < 0$ and negative permittivity $\varepsilon < 0$ [3]. One of the ground-breaking applications of the negative refractive index lies in the fact

that it can be used to construct a superlens, a negative-refractive lens, to focus electromagnetic waves at a desired range of frequencies [4].

There have been numerous explorations on using superlens for exciting purposes such as constructing subwavelength images (providing the image of two light sources that are separated by an interval smaller than the used wavelength) [5] and transferring wireless energy [6]. More recently, the use of metamaterials in energy harvesting has become an attractive research topic [7,8]. It is known that properly designed metamaterials can absorb and possibly transform electromagnetic energy in the ambient to electric currents as a source of cheap and renewable energy [9]. The motivation of ultilizing metamaterials in energy harvesting is to capture, store, and reuse the energy in those waves, rather than losing it to the environment. This can be done by the implementation of metamaterial absorbers, for instance, to make batteries powered by wireless GHz hotspots [10] as illustrated in Fig. 1(a). However, the applicability of energy harvesting devices based on metamaterial absorbers has been seriously challenged by the fact that the electromagnetic energy rapidly decays in the space due to divergence of the beam and absorption in the air. In the other words, the energy harvesting is effective only if the distance between the source and the absorber is short. While the original form of the superlens is flat so that it can focus the electromagnetic energy from a source at infinity, later studies have shown that the geometric form of negative-refractive superlens can be arbitrarily designed for various purposes. In this work we propose a metamaterial-based superlens operating as an amplifier for electromagnetic waves in the GHz regime. As shown in Fig. 1(b), if the microwave electromagnetic waves are emitted from a source at infinity, the energy absorbed by small-surface metamaterial absorbers can be greatly enhanced by focusing the electromagnetic waves using a concave negative-refractive superlens. The negative refractive nature of the superlens is numerically analyzed using the finite integration simulation technique. The wave propagation and energy distribution in space, with and without the superlens, are simulated to elaborate our idea.

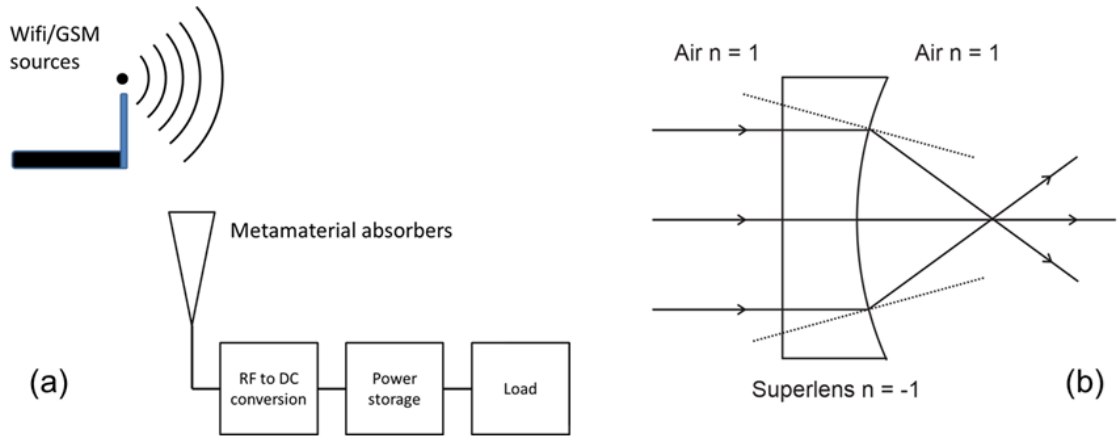

Figure 1. (a) A schematic drawing of an energy harvesting device using metamaterial absorbers and (b) an ideal case of wave propagation from a source at infinity through a concave negative-refractive superlens.

2. SIMULATION SETUP

The proposed metamaterial is composed of periodically-arranged double-sided fishnet structures, whose unit cell consists of paired disks merged with crossed continuous wires as shown in Fig. 2(a). The lattice parameter, the width of the wire, and the radius of the disk are

defined as *a*, *w*, and *R*, respectively. The front and back metallic patterns are separated by a dielectric substrate. The used dielectric material is commercial-type Duroid 5880 with a thickness of 0.25 mm. Copper is selected as the metal material with a 17.5 μm thickness. It should be noted that the choice of the dielectric substrate material has a significant impact on the efficiency of the negative index metamaterial since the substrate losses dramatically influence the transmission of the whole structure [11]. For this reason, the Duroid material with a relative dielectric constant $\varepsilon_r = 2.2$ is chosen. It has a small tangent $\delta = 0.0009$ at microwave frequencies. In this study, we consider a negative-refractive metamaterial operating at 36-42 GHz. To address this frequency range the unit cell has a periodicity *a* of 4.9 mm, while the metal slabs have a width *w* of 1.45 mm and a disk radius *R* of 2.3 mm. Due to the symmetric configuration, the structure works for arbitrary linear polarizations. The propagation direction of the incident electromagnetic wave is perpendicular to the metamaterial surface. Shifting the working frequency for a particular emitted source can be easily adapted by the well-known frequency-dimension scalability of metamaterials [12].

In the following, the results are divided into two parts. In a first series of simulations, we characterize the negative refractive index of the fishnet metamaterial structure. The electromagnetic simulations are performed by CST Microwave Studio with the finite-integration technique [13]. The unit cell is placed between two waveguide ports, which act like the transmitter and receiver antennas with periodic boundary conditions. In the second series of simulations, the concave negative-refractive superlens is composed by stacking metamaterial layers in descending order from the left and right sides to the center. Two concave superlens with different radius as illustrated in Figs. 2(b) and 2(c) are considered to show how we control the focal point of the electromagnetic energy. These two superlens have the same length $L = 93.1$ mm but different radius, r_1 of 73.8 mm corresponding to a height H_1 of 5.2 mm [Fig. 2(b)] and r_2 of 36.1 mm corresponding to a height H_2 of 9.4 mm [Fig. 2(c)], for long and short focal points, respectively. The source at infinity is simulated by a plane wave and guided by a perfectly electric conducting waveguide.

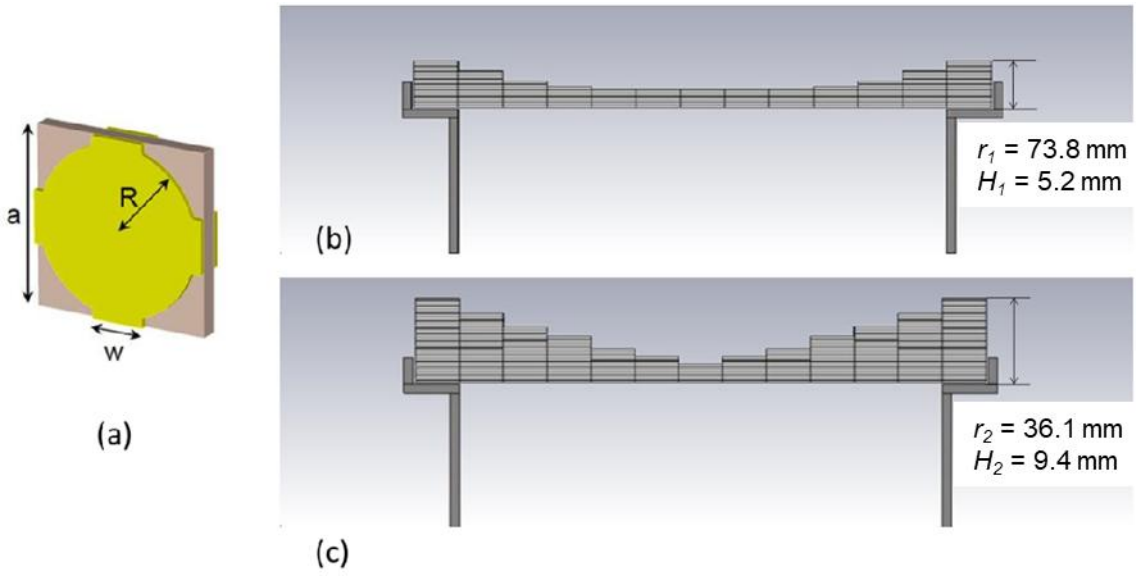

Figure 2. (a) Computational unit cell of the negative-refractive metamaterials and the corresponding metamaterial superlens with radii of (b) 73.8 and (c) 36.1 mm (heights of 5.2 and 9.4 mm, respectively).

The final aim of two simulation series is to demonstrate that the microwave radiation emitted from a source at infinity can be amplified after passing through a negative-refractive superlens. For focusing of the radiation beam, the incident waves are required to travel through a phase correction and amplitude amplification process. The metamaterial negative-refractive superlens provides both phase correction and amplitude amplification of the waves [14]. In our simulation setup, the position of the superlens is 16 mm away from the plane-wave port in the z direction. With the concave geometry of the negative-refractive superlens, one can expect that the refraction beam inside the superlens will be on the same side with the incident beam and the electromagnetic energy can be focused at a certain point as illustrated in Fig. 1(b). By changing the radius of the concave geometry, the beam's convergence distance, and consequently the distance between the source and the focusing point, can be controlled.

3. RESULTS AND DISCUSSION

3.1. The negative refractive index of metamaterials

The purposes of this section are i) to demonstrate the negativity of the refractive index of the proposed fishnet metamaterials, which is the key factor to build the superlens; and ii) to maximize the applicability of the proposed metamaterial by optimizing the transmission at the negative refractive frequency. The higher the transmission, the more energy is sent through the superlens, and the greater the signal amplification factor. Therefore, we have determined the transmission and reflectance of the fishnet structure. Complex frequency dependent S-parameters, S_{11} and S_{21}, were obtained from simulations. The transmission $T(\omega)$ is equal to $|S_{21}|^2$ and the reflection $R(\omega)$ is equal to $|S_{11}|^2$.

Fig.3 shows the simulation results of the transmission-optimized metamaterial. To optimize transmission, the free space and metamaterial impedance must be equal [15]. The condition for the optimal impedance of the material is given by the formula:

$$Z = \sqrt{\frac{\mu}{\varepsilon}} = 1. \tag{1}$$

Since μ is often fixed by the magnetic resonant frequency, it is more convenient to tune ε for matching with μ by shifting the plasma frequency of the continuous metal wires as [15,16]:

$$f_p^2 = \frac{c_0^2}{2\pi d^2 \ln\frac{d}{w}}, \tag{2}$$

where f_p is the plasma frequency, d is the distance between two wires, w is the width of the wire, and c_o is the speed of light in vacuum. During the optimization process, we adjusted the width of the continuous wires (not shown here) to tune permittivity and permeability for impedance matching.

The optimized transmission and reflection spectra are plotted in Fig. 3(a). Fig. 3(b) presents the permittivity, permeability, and refractive index for a single layer of fishnet metamaterials, which are extracted from the scattering parameters by the standard retrieval procedure [17]. It is clear that a negative value of the refractive index emerges from 36 GHz to 42 GHz with the highest transmission being 0.8 at 37 GHz. In the superlens, due to the strong interaction between metamaterial layers, the overlap between the negative permittivity and negative permeability changes and consequently, the negative refractive band is slightly shifted. The highest

transmission is found around 39 GHz for the superlens. Therefore, to examine the amplifying ability of the negative-refractive superlens, we consider its functionality at the frequency of 39 GHz.

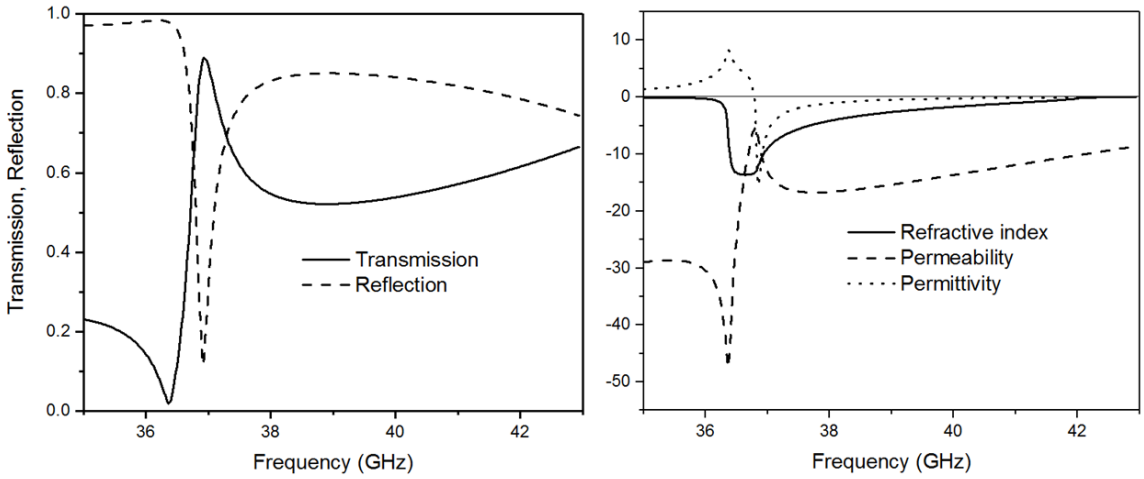

Figure 3. (a) Transmission and reflection of the fishnet structure. (b) The effective refractive index, permittivity, and permeability. $n = 0$ is represented by a thin solid line.

3.2. Energy focusing

The electromagnetic waves propagating in free space are simulated and their electric field intensity is presented in Fig. 4(a). As one might expect, the farther away from the source, the lower the field intensity. As comparison, Fig. 4(b) shows the situation in which the superlens with large radius (r_1 = 73.8 mm, H_1 = 5.2 mm) is used. It can be seen that the waves converge at a focusing area before diverging again. Due to imperfectness of the concave geometry, the electromagnetic waves cannot be focused into a point as expected. The divergence observed after the converging range is consistent with the prediction. The distributions of electric field intensity along the propagation direction with and without the superlens are shown in Fig.4(c) for comparison. It is obvious that the electric field intensity is greatly enhanced by the superlens. In particular, using the superlens the electric field intensity is 6.3 times stronger at 90 mm (the focal point) away from the port (corresponding to about 74 mm from the superlens) compared with the case without superlens.

In principal, the focal length can be controlled by properly selecting the lens radius. Figure 5 shows the relation between the focal length, the refractive index, and the lens radius. As can be seen, the large radius superlens (r_1 = 73.8 mm, H_1 = 5.2 mm) has a focal length f_1 = 71.6 mm, while the small radius superlens (r_2 = 36.1 mm, H_2 = 9.4 mm) has a focal length f_2 = 35.8 mm. In this case, we can use the classical Lensmaker's equation with negative value of n to describe the relation between f, r, and n:

$$\frac{1}{f} = (n-1)\left(\frac{1}{r} + \frac{1}{r_{back}}\right) \tag{3}$$

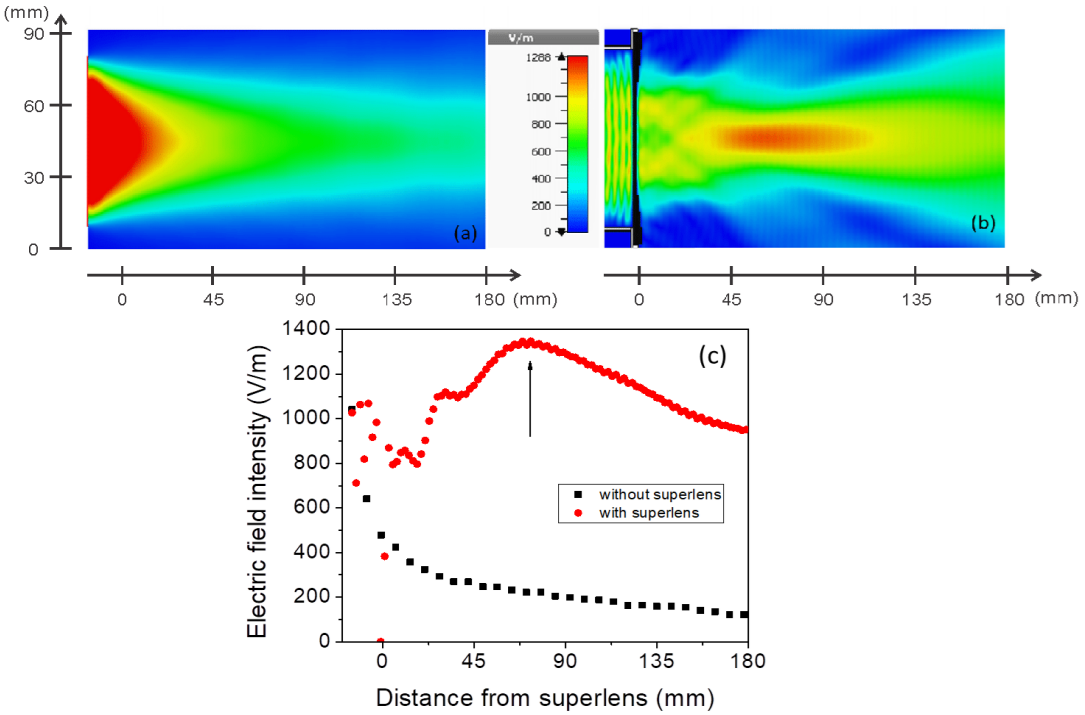

Figure 4. Distribution maps of electric field intensity for the propagation of 39 GHz wave in the z-direction (a) in free space and (b) with superlens (r_1 = 73.8 mm, H_1 = 5.2 mm). (c) The difference between time-average electric field intensity distributed at the centre of the z-direction with and without the superlens.

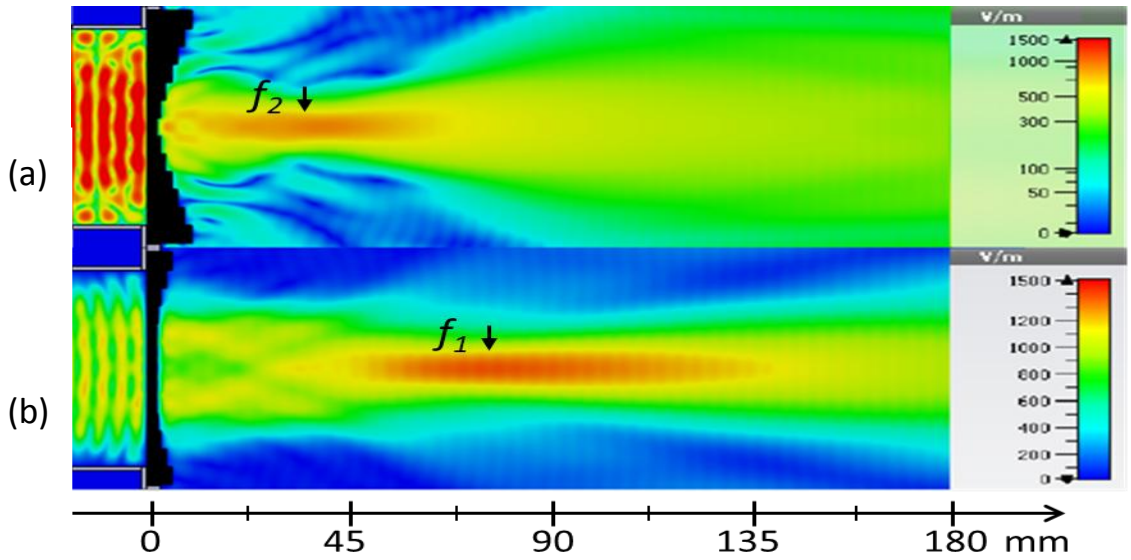

Figure 5. Distribution maps of the electric field intensity at 39 GHz for negative-refractive superlenses with two different concave radius corresponding to (a) r_2 = 36.1 mm (small radius) and (b) r_1 = 73.8 mm (large radius). The higher intensity for z<0 in (a) is related to the larger reflection by the superlens given the larger number of layers.

In this case $r_{back} = \infty$, so the focal length scales linear with the front radius r of the superlens. The values of (negative) n determined for the two superlenses using Eq. (3) are in good agreement: n_1 = -2.03 and n_2 = -2.01. It is confirmed that the different shapes of superlenses have almost no effect on their refractive index, but considerably alter the focal length.

4. CONCLUSIONS

We have demonstrated that it is possible to design microwave metamaterial-based superlens operating at the microwave frequency range. It is shown that using the proposed superlens the microwave electromagnetic from a source at infinity can be greatly amplified at a certain area. In our simulations, the focused electric field intensity is 6 times greater than that the original one. In addition, we have shown that the focal length can controlled by changing the concave radius of the superlens. These findings put a solid step toward the experimental demonstration of superlenses for promising applications in wireless power transmission and wifi energy harvesting.

***Acknowledgement*:** This research is funded by Vietnam National Foundation for Science and Technology Development (NAFOSTED) under grant number FWO.103.2017.01, Vietnam Academy of Science and Technology under grant number KHCBVL.01/18-19, and National Key Laboratory of Electronic Materials and Devices, Institute of Materials Science under grant number CSTĐ.02.18.

REFERENCES

1. Soukoulis C. M. and Wegener M. - Past achievements and future challenges in the development of three-dimensional photonic metamaterials, Nature Photon **5** (2011) 523-530.
2. Schurig D., Mock J., Justice B., Cummer S. A., Pendry J. B., Starr A. and Smith D. - Metamaterial Electromagnetic Cloak at Microwave Frequencies, Science **314** (2006) 977-980.
3. Veselago V. G. - The electrodynamics of substances with simultaneously negative values of ε and μ, Physics-Uspekhi **10** (1968) 509-514.
4. Pendry J. B. - Negative Refraction Makes a Perfect Lens, Phys. Rev. Lett. **85** (2000) 3966.
5. Chen W. T., Zhu A. Y., Sanjeev V., Khorasaninejad M., Shi Z., Lee E., and Capasso F. - A broadband achromatic metalens for focusing and imaging in the visible, Nature Nanotech, **13** (2018) 220-226.
6. Lipworth G., Ensworth J., Seetharam K., Huang D., Lee J. S., Schmalenberg P., Nomura T., Reynolds M. S., Smith D. R., and Urzhumov Y. - Magnetic Metamaterial Superlens for Increased Range Wireless Power Transfer, Sci. Rep. **4** (2014) 3642.
7. Wang Y., Sun T., Paudel T., Zhang Y., Ren Z., Kempa K. - Metamaterial plasmonic absorber structure for high efficiency amorphous silicon solar cells, Nano Lett. **12** (2011) 440-445.
8. Alavikia B., Almoneef T. S., and Ramahi O. M. - Complementary split ring resonator arrays for electromagnetic energy harvesting, Appl. Phys. Lett. **107** (2015) 033902.

9. Thang N. M., Anh D. T., Viet D. T. and Tung N. T. - New generation of electromagnectic absorbing Metamaterial , Journal of Military Science and Technology **55**th Anniversary of Journal (2015) 303-309 (in Vietnamese).
10. Alshareef M. and Ramahi O. M. - Electrically small resonators for energy harvesting in the infrared regime, J. Appl. Phys. **114** (2013) 223101.
11. Tung N. T., Lam V. D., Cho M. H., Park J. W., Jang W. H., and Lee Y. P. - Influence of the dielectric-spacer thickness on the left-handed behavior of fishnet metamaterial structure, Photon Nanostruct: Fundamentals and Applications **7** (2009) 206-211.
12. Tien P. D., Le L. N., Nhan P. T., Tung N. T., and Thang N. M. - Linear geometry frequency scalability in metamaterial absorbers, Journal of Military Science and Technology **49** (2017) 161-166 (in Vietnamese).
13. www.cst.com, accessed May 23, 2018.
14. Aydin K., Li Z., Sahin L. and Ozbay E. - Negative phase advance in polarization independent, multi-layer negative-index metamaterials, Opt. Express **16** (2008) 8835-8844.
15. Tung N. T., Hoai T. X., Lam V. D., Park J. W., Thuy V. T., and Lee Y. P. - Perfect impedance-matched left-handed behavior in combined metamaterial, Eur. Phys. J. B **74** (2010) 47-51.
16. J. B. Pendry, A. J. Holden, W. J. Stewart, and I. Youngs - Extremely low frequency plasmons in metallic mesostructures, Phys. Rev. Lett. **76** (1996) 4773.
17. Tung N. H., Le B. H., Trang P. T., Hai L. D., Lam V. D., and Tung N. T. - A combined solution for determination of multi-branched refractive index in 1D metamaterials, Journal of Military Science and Technology **38** (2015) 110 (in Vietnamese).